This is the accepted manuscript made available via CHORUS. The article has been published as:

# Effects of charge inhomogeneities on elementary excitations in La_{2−x}Sr_{x}CuO_{4}

S. R. Park, A. Hamann, L. Pintschovius, D. Lamago, G. Khaliullin, M. Fujita, K. Yamada, G. D. Gu, J. M. Tranquada, and D. Reznik

Phys. Rev. B **84**, 214516 — Published 12 December 2011

DOI: 10.1103/PhysRevB.84.214516

# Effects of charge inhomogeneities on elementary excitations in $La_{2-x}Sr_xCuO_4$

S. R. Park[1], A. Hamann[2], L. Pintschovius[2], D. Lamago[2,3], G. Khaliullin[4],
M. Fujita[5], K. Yamada[6], G. D. Gu[7], J. M. Tranquada[7], D. Reznik[1*]
[1]*Department of physics, University of Colorado at Boulder, Boulder, Colorado, USA*
[2]*Karlsruher Institute für Technologie, Institute für Festkörperphysik, P.O. Box 3640, D-76021 Karlsruhe, Germany*
[3]*Laboratoire Leon Brillouin, CEA-Saclay, F-91191 Gif sur Yvette Cedex, France*
[4]*Max-Planck-Institut für Festkörperforschung, Heisenbergstrasse 1, D-70569 Stuttgart, Germany*
[5]*Institute for Materials Research, Tohoku University, Senda, Miyagi 980-8577, Japan*
[6]*IWPI Research Center, Advanced Institute for Materials Research,*
*Tohoku University, Sendai 980-8577, Japan and*
[7]*Condensed Matter Physics & Materials Science Department,*
*Brookhaven National Laboratory, Upton, New York 11973, USA*
(Dated: October 19, 2011)

Purely local experimental probes of many copper oxide superconductors show that their electronic states are inhomogeneous in real space. For example, scanning tunneling spectroscopic (STS) imaging shows strong variations in real space, and according to nuclear quadrupole resonance (NQR) studies the charge distribution in the bulk varies on the nanoscale. However, the analysis of the experimental results utilizing spatially-averaged probes often ignores this fact. We have performed a detailed investigation of the doping-dependence of the energy and line width and position of the zone-boundary Cu-O bond-stretching vibration in $La_{2-x}Sr_xCuO_4$ by inelastic neutron scattering. Both our new results as well as previously reported angle-dependent momentum widths of the electronic spectral function detected by angle-resolved photoemission can be reproduced by including the same distribution of local environments extracted from the NQR analysis.

PACS numbers: 63.20.-e, 74.25.Kc, 63.50.-x

## I. INTRODUCTION

It is by now recognized that charge inhomogeneity is an important aspect of copper oxide superconductors. Undoped copper oxygen planes are Mott insulators due to a strong on-site Coulomb interaction. They become metallic and exhibit high-temperature superconductivity (HTSC), when they are doped.[1] Different types of charge inhomogeneity can emerge as a result of doping. Nanoscale inhomogeneity due to strong correlations between electrons, such as a stripe or checkerboard order[2,3], received a lot of attention in recent years.[4–6] Other sources of inhomogeneity are randomly distributed heterovalent substituents or extra oxygen atoms, which introduce doped holes or electrons into the copper oxygen planes.[7,8] In most cases (with some notable exceptions, such as Ortho II-ordered $YBa_2Cu_3O_{6.5}$), the dopants act as charged impurities. They form an inhomogeneous Coulomb potential impacting the conduction electrons in the copper oxygen planes, resulting in an inhomogeneous charge distribution. Local probes such as scanning tunneling microscopy (STM) have provided evidence for this inhomogeneity in cuprates such as $Bi_2Sr_2CaCu_2O_{8+x}$ (BSCCO),[9–12] $Ca_{2-x}Na_xCuO_2Cl_2$,[13] and $La_{2-x}Sr_xCuO_4$ (LSCO).[14] Bulk-sensitive nuclear magnetic resonance (NMR) and nuclear quadropole resonance (NQR) experiments confirmed that an inhomogeneous charge distribution is not just a property of the surface, but is a feature of the bulk in LSCO.[15–17]

Here we show how some doping-dependent features of the observed spectra of phonons and electronic quasiparticles in LSCO, can be naturally explained in terms of an inhomogeneous charge distribution. For phonons, we base our analysis on new results of neutron scattering experiments presented here. We use previously published angle resolved photoemission (ARPES) data for the electronic response.

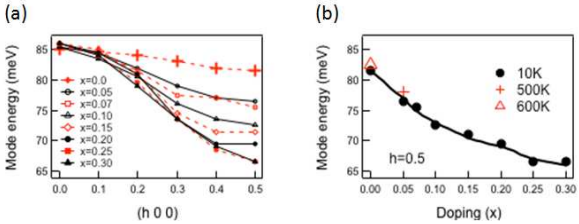


FIG. 1: Doping dependence of the Cu-O bond-stretching mode energy. a) Dispersion in the [100]-direction at different doping levels. b) Zone boundary half-breathing ($h = 0.5$) mode energy as a function of doping (x).

It is a long-standing observation that the energy of the zone boundary Cu-O bond-stretching (half-breathing) phonon, $\mathbf{q} = (0.5, 0, 0)$, depends strongly on doping. It changes from about 81 meV at $x = 0$ to about 67 meV at $x = 0.3$.[18–20] Figure 1(b), which combines previous neutron scattering and x-ray scattering data with our new results for the frequency of the half-breathing mode, summarizes the available data. Since the phonon frequency depends strongly on the doping, especially in the underdoped region, an inhomogeneous doping should increase its observed line width. We have measured the line width of this phonon in the underdoped region to investigate this effect.

## II. EXPERIMENTAL DETAILS

Inelastic neutron scattering experiments were performed on large, high-quality single crystals of LSCO with $x = 0$, 0.05, 0.07, and 0.15 on the 1T triple axis spectrometer at the ORPHEE reactor at the Laboratoire Leon Brillouin at Saclay, France. The monochromator and analyzer were the (220) reflection of Copper and the (002) reflection of pyrolytic graphite (PG), respectively. The measurements were performed at reciprocal lattice vectors $\mathbf{Q} = (4 + h, 0, 0)$ in the tetragonal notation. In order to measure the intrinsic phonon line width, it is important to properly account for the experimental resolution, which depends not only on the instrument configuration, but also on the phonon dispersion in the vicinity of the measured point in $\mathbf{Q}$-$\omega$ space. We calculated the effective energy-resolution for the bond-stretching phonon branch at each doping level based on the spectrometer resolution combined with doping-dependent dispersions calculated from the shell model, whose parameters were optimized to agree with previously published phonon dispersion data along high symmetry directions.[21] The calculated experimental resolutions at Q=(4.5, 0, 0) for x=0.0, x=0.05, x=0.07 and x=0.15 are 4.5, 3.6, 3.2 and 3.4 meV, respectively. Electron-phonon coupling or anharmonicity should result in a Lorentzian intrinsic phonon line shape, but we found that a Gaussian gives better fits. Thus, the resolution function was convolved with a Gaussian function representing the phonon peak, with the Gaussian width (and frequency and amplitude) determined by fitting to a constant-$\mathbf{Q}$ scan. The background was determined from the scans at nearby wave vectors as was done in Ref. 22

## III. RESULTS AND DISCUSSION

Figure 2(a-d) shows inelastic neutron scattering (INS) spectra of the half-breathing mode of LSCO from $x = 0$ to $x = 0.15$. The frequency clearly softens with increasing doping, as previously reported.[18] Red lines through the raw data indicate the fitted Gaussian peak, convolved with the resolution function, on top of a linear background. In the cases of $x = 0.0$ and $x = 0.05$, we have included a second Gaussian to account for a small peak at 87 meV that we believe corresponds to an artifact,[23] based on its lack of dependence on doping, although we do not have a definitive explanation for it. We will ignore it in the following discussion of the line width; including it in the evaluation of the line width would not make a qualitative difference to the argument, as discussed below.

The fitted phonon line widths are plotted as a function of doping in Fig. 2(f). The filled symbols show the width of the half-breathing mode at low temperature. As one can see, the width makes a large jump from $x = 0$ to $x = 0.05$, and then gradually decreases with further doping. For comparison, the open diamonds show the fitted width

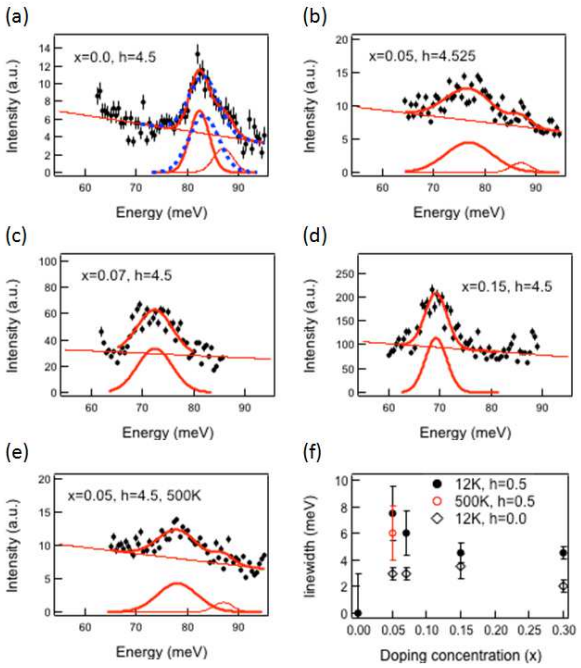


FIG. 2: Inelastic neutron scattering data of half breathing zone boundary bond-stretching modes in LSCO. a) $x = 0$, b) $x = 0.05$, c) $x = 0.07$, d) $x = 0.15$ at 10 K, and e) $x = 0.05$ at 500 K. Red lines on raw data are composed of a linear background and two Gaussian peaks for (a) and (b) and a linear background and a Gaussian peak for (c), (d) and (e). Large Gaussian peaks on the bottom represent longitudinal bond-stretching modes; small Gaussian peaks at 87 meV represent the a suspect artifact (see text). Full widths of half maximum (FWHM) of the main peaks of x=0, x=0.05, x=0.07 and x=0.15 are 4.5 meV, 10.5 meV, 8 meV and 5meV, respectively. Two Gaussian peaks of x=0.0 data and a small Gaussian peak of $x = 0.05$ data are resolution-limited (4.5 meV). Dotted blue line on $x = 0.0$ raw data is composed of a linear background and a Gaussian peak with 6.5 meV FWHM. f) Doping dependence of the zone boundary ($h = 0.5$) and zone center ($h = 0.0$) longitudinal bond-stretching mode line widths after deconvolving the resolution function.

of the zone-center mode. The absence of any significant variation with doping suggests that the results for $h = 0.5$ are intrinsic and are not a result of difference in sample quality. Furthermore, different samples with the same doping give identical results.

The most obvious explanation of phonon broadening at the zone boundary is electron-phonon coupling. According to the conventional theory of metals, the phonon line width due to electron-phonon coupling should be proportional to the density of states near $E_F$,[25,26] which is roughly proportional to doping in LSCO.[27–29] The trend for the $h = 0.5$ mode in Fig. 2(f) clearly violates a simple monotonic increase with doping. In particular, the $x = 0.05$ sample is insulating[30] and should not have more conduction electrons near the Fermi surface than the $x = 0.07$ and 0.15 samples. Thus, we can rule out electron-phonon coupling as the dominant cause of this

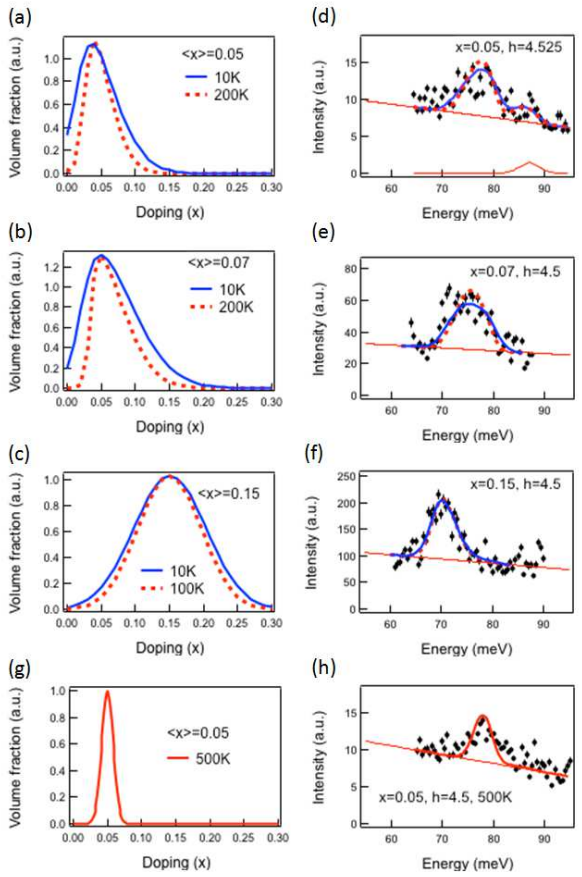


FIG. 3: Doping distributions for $x = 0.05$ (a and g), $x = 0.074$ (b) and $x = 0.15$ (c) based on the NQR data.[15] Inelastic neutron scattering data from the half-breathing mode for $x = 0.05$ (d), $x = 0.07$ (e) and $x = 0.15$ (f) at 10 K and $x = 0.05$ at 500 K (h). Dotted red curves and solid blue curves over data points show results calculated from the inhomogeneous doping effect at high temperature and at 10 K, respectively. Red curve in (h) shows the simulated results at 500 K.

effect.

Another possible explanation of the broadening of the low-temperature line shape is the effect of the tilt of the $CuO_6$ octahedra responsible for the transition from the high-temperature tetragonal to the low-temperature orthorhombic phase.[31] We can rule out this scenario because octahedral tilt is largest for $x = 0$ and decreases with doping.

Here we propose a different mechanism to explain our results. As already mentioned, NQR and NMR experiments found that the doping level in nominally homogeneous samples of the LSCO family is strongly spatially inhomogeneous.[15,16] Since the phonon frequency is known to depend on doping, as shown in Fig. 1, we propose that the observed broadening results from the distribution of local environments observed by NQR. To test this idea we modeled phonon line shapes based on the distribution of dopings measured by NQR[15] combined with the doping dependence of phonon frequencies. (As the intrinsic phonon line-width is smaller than the resolution, we have ignored it in the modeling.) The resulting line shapes were convolved with the resolution function. This analysis provides a very rigorous test of the above hypothesis, since it contains no adjustable parameters aside from the overall peak magnitude.

One can imagine more rigorous approaches to calculate the phonon spectrum in an inhomogeneous medium such as calculations based on the coherent potential approximation (CPA) which is usually used for calculating phonon spectra in alloys.[32] But it is not clear if this method would apply to phonons in solids with charge inhomogeneity as in LSCO, since the CPA was originally developed for random, mass disordered alloys.[32] However, we note that calculations of disorder effects in isotopically disordered Ge using CPA gave no better results (actually even slightly inferior results) than calculations using large supercells.[33] Somewhat surprisingly, the supercell approach reproduced the experimentally observed phonon frequencies, linewidths and intensities very well, in spite of the fact that this approach is based on harmonic lattice dynamics. Therefore we think that our ansatz for calculating linewidths in LSCO - which is equivalent to a simplified version of the supercell approach - is quite adequate.

Figure 3 shows that the calculated line shapes reproduce the experimental low temperature phonon line shapes at three doping levels reasonably well. We also measured this phonon in the $x = 0.05$ sample at 500 K. Heating to such temperatures increases anharmonicity and thus broadens the phonon. For example, this broadening has been observed already at 330 K near the zone center in similar samples.[35] However, the 500-K data appear to be slightly narrower than at 10 K, which is consistent with decreasing charge inhomogeneity with increasing temperature as reported by NQR.[15] An anharmonic contribution must be present, but it appears to be comparable to the contribution from charge inhomogeneity.

It is not completely clear why charge inhomogeneity decreases upon heating the sample. One possibility is that some electrons are trapped by the disordered chemical potential due to randomly distributed Sr cations.[15] Then, the real space distribution of the trapped electrons should broaden with increasing temperature resulting in a smoother disorder potential.[15] Charge inhomogeneity resulting from electronic correlations should also decrease at elevated temperatures due to the breakup of electronic self-organization by thermal fluctuations.

Based on the above evidence we conclude that the phonon linewidth can be well explained by charge inhomogeneities measured by NQR. Intrinsic phonon lifetime, which is governed by anharmonicity and electron-phonon coupling, is too long to measurably contribute to the linewidth in addition to the effect of inhomogeneous doping.

If this explanation is correct, charge inhomogeneity should show up in other experiments involving spatially-averaged probes. In particular, electronic quasiparti-

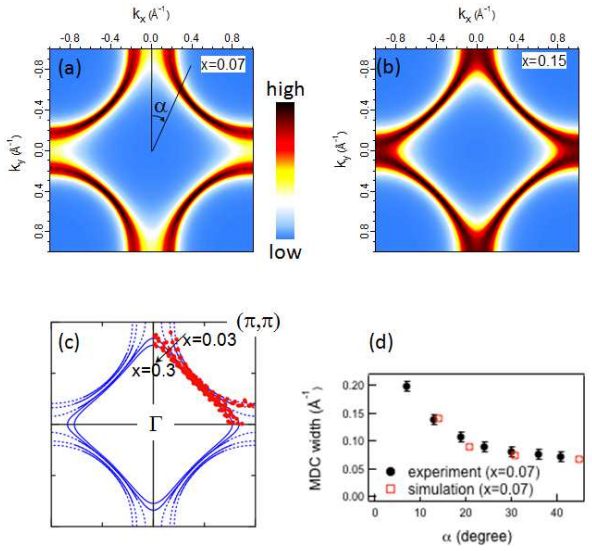


FIG. 4: Simulated Fermi surface results for (a) $x = 0.07$ and (b) $x = 0.15$. (c) Doping dependent Fermi surface evolution extracted from the ARPES data.[29] (d) MDC widths at Fermi energy from experiment[36] and simulation from anti-nodes to nodes.

cles measured by ARPES should also be affected by inhomogeneous doping, since the Fermi surface in LSCO has a strong and nontrivial doping dependence: The Fermi wave vector $\mathbf{k}_f$ is nearly doping-independent at the nodes, but rapidly decreases with increased doping near the antinodes due to the proximity to a Van Hove singularity (Fig. 4c).[29,37] Similarly, measurements of the momentum width of the spectral function obtained from momentum distribution curves (MDCs) show that the width at the Fermi level is substantially larger in the antinodal region compared to the nodal one.[36,38] We find that combining the chemical-potential-distribution model with the observed doping dependence of $\mathbf{k}_f$ provides a reasonable explanation for the $\mathbf{k}$ dependence of the momentum widths.

Figure 4(c) shows the doping-dependent Fermi surfaces extracted from the ARPES data[29]. We simulate the ARPES data by introducing a Lorentzian broadening in energy of $\Delta E = 70$ meV FWHM, which translates into $\Delta E/v_F$, broadening in $\mathbf{k}$, at each $\mathbf{k}$-point and assuming a distribution of the electronic band structures weighted by the inhomogeneous doping distribution, as we had done for the zone boundary phonon. 70 meV FWHM is a reasonable value based on the measured quasiparticle peak width near the Fermi energy in LSCO.[39] We use tight binding bands with first, second and third neighbor hopping parameters fitted to the ARPES data as the electronic band structures for each doping.[36] Figure 4(a) and (b) show the simulated results for the Fermi surfaces of $x = 0.07$ and $x = 0.15$, respectively. Momentum widths of the quasiparticles near the Fermi surface broaden on going from the nodal to the anti-nodal directions for both dopings, as observed in experiments.[40]

Figure 4(d) demonstrates a good quantitative agreement between the MDC widths calculated from our model and the data[36] for $x = 0.07$. The line width of ARPES data at the Fermi energy has been, so far, usually interpreted as the self-energy effect of the quasiparticle due to impurity scattering. There is, however, no reason that the line width near anti-nodal direction is much broader than the line width near nodal direction due to impurity scattering which is believed to be isotropic. Our new analysis, yet, provides a natural explanation about broader line width near anti-nodal direction.

An alternative model is to apply a broadening of fixed width in momentum rather than energy; however, it was found that uniform momentum broadening gives a much poorer agreement with the data. The physical significance of this result is unclear.

Broader ARPES line widths near the anti-nodal directions have been interpreted in terms of stronger scattering,[40] but we quantitatively reproduced the experimental data with a large enhancement of the MDC widths towards the anti-nodal direction by the inhomogeneous doping effect. Our simulation, which only includes doping inhomogeneity, cannot reproduce the entire ARPES spectrum, especially in the anti-nodal region, because of the pseudogap and the incoherent spectrum at higher binding energies.[41] However, we can conclude that the long-standing observation of broader peaks near antinodes in LSCO is due, in large part, to inhomogeneous doping. We find further evidence for the mechanism proposed here from another cuprate superconductor. Quantum oscillation measurements showed that an overdoped $Tl_2Ba_2CuO_{6+d}$ (Tl2201) has a much more homogenous chemical potential,[42] because the dopants in Tl2201 are farther from the copper oxide plane than the dopants in LSCO and BSCCO.[7] Recent ARPES data on this material show that the spectral functions near the anti-nodes are even sharper than those at the nodes.[43] These results are consistent with the conclusion that the broader lineshape near the anti-node than near the node is not universal in the cuprates but is a material dependent effect resulting from doping inhomogeneities.

Crystal momentum is generally a good quantum number for the electronic quasiparticles, whereas the length scale of charge inhomogeneities in real space is only a few nanometers.[9,12–15] Thus, it may be surprising that the spectra of phonons and of the electronic quasiparticles are well reproduced by a linear sum of spectral peaks for each doping weighted by the inhomogeneous doping distribution function. For the electronic quasiparticles, 70 meV FWHM intrinsic line width, combined with the measured Fermi velocity, translates into about 3 nm mean free path for the nodal direction, which is almost the same as the length scale of doping variation from NQR[15] and STM.[14] It is even shorter for the antinodal quasiparticles, because they have a smaller Fermi velocity. We can, therefore, think that electronic quasiparticles reside in each patch, and simply add all spectral peaks from corresponding patches with different dopings.

For the phonon, we do not need additional line width broadening to fit the experimental data as shown in Fig. 3. This, however, does not mean that the phonon has a much longer correlation length than the electronic quasiparticles. If the wavelength of any waves in an inhomogeneous medium is smaller than the length scale of the inhomogeneity of the medium, the waves tend to be localized inside a domain of the inhomogeneous medium.[44–47] The wavelength of zone boundary phonons is two unit cells, which is about 4 times shorter than the length scale of the inhomogeneity measured by STM and NQR.[14,15] Thus the distribution of the zone boundary phonon frequencies in a medium with inhomogeneous force constants directly reflects the distribution of the force constants.

To summarize, we have found evidence that elementary excitations in LSCO such as phonons and electronic quasi-particles, are strongly influenced by inhomogeneous doping previously reported by purely local probes, NQR, NMR, and STM. Phonon and electronic spectra are well reproduced by just averaging over spectra from patches having various doping concentrations, even though the typical length scale of a patch is a few nanometers. Good agreement between the model based on inhomogeneous doping with both ARPES and neutron results despite almost no adjustable parameters, provides compelling evidence that inhomogeneous doping must be included into any analysis of experimental results in the cuprates. Recently, iron pnictide superconductors have also turned out to have chemical potential inhomogeneities due to a random dopant distribution.[48] It is, therefore, necessary to take account of these charge inhomogeneities when interpreting measurements on iron pnictide superconductors as well.

Inhomogeneity most likely originates from a random potential created by introduced dopants (in LSCO it would be Sr), rather than from the self-organization of conduction electrons, for example into stripes. It is, yet, essential to gain further insight into interactions of dynamic stripes with phonons, which is at the focus of a different project. If stripes interact with phonons via a mechanism discussed in Ref. 35,49, then the effect of dynamic stripes should occur at a different wave vector, $\mathbf{q} = (0.25, 0, 0)$, not at the zone boundary. In fact we find that the huge phonon line widths reported near this wave vector in Ref. 35 cannot be reproduced by inhomogeneous doping alone for $x \geq 0.07$, and large additional broadening is required near optimal doping. These results will be presented in a subsequent publication.

### Acknowledgments

The work at the University of Colorado was supported by the DOE, Office of Basic Energy Sciences under Contract No. DE-SC0006939. GDG and JMT are supported at Brookhaven by the Office of Basic Energy Sciences, Division of Materials Science and Engineering, U.S. Department of Energy (DOE), under Contract No. DE-AC02-98CH10886. The work at Tohoku University was supported by the Grant-In-Aid for Science Research A (22244039) from the MEXT of Japan.

* Electronic address: dmitry.reznik@colorado.edu

[1] Patrick A. Lee, Naoto Nagaosa and Xiao-Gang Wen, Rev. Mod. Phys. **78**, 17 (2006).

[2] V. J. Emery, S. A. Kivelson, and H. Q. Lin, Phys. Rev. Lett. **64**, 475 (1990).

[3] J. Zaanen and O. Gunnarsson, Phys. Rev. B **40** 7391 (1989).

[4] J. M. Tranquada, B. J. Sternlieb, J. D. Axe, Y. Nakamura and S. Uchida, Nature **375**, 561 (1995).

[5] P. Abbamonte, A. Rusydi, S. Smadici, G. D. Gu, G. A. Sawatzky and D. L. Feng, Nat. Phys. **1**, 155 (2005).

[6] T. Hanaguri, C. Lupien, Y. Kohsaka, D.-H. Lee, M. Azuma, M. Takano, H. Takagi and J. C. Davis, Nature **430**, 1001 (2004).

[7] H. Eisaki, N. Kaneko, D. L. Feng, A. Damascelli, P. K. Mang, K. M. Shen, Z.-X. Shen and M. Greven, Phys. Rev. B **69**, 064512 (2004).

[8] Michela Fratini, Nicola Poccia, Alessandro Ricci, Gaetano Campi, Manfred Burghammer, Gabriel Aeppli and Antonio Bianconi, Nature **466**, 841 (2010).

[9] S. H. Pan, J. P. O'Neal, R. L. Badzey, C. Chamon, H. Ding, J. R. Engelbrecht, Z. Wang, H. Eisaki, S. Uchida, A. K. Gupta, K.-W. Ng, E. W. Hudson, K. M. Lang and J. C. Davis, Nature **413**, 282 (2001).

[10] K. McElroy, J. Lee, J. A. Slezak, D.-H. Lee, H. Eisaki, S. Uchida, and J. C. Davis, Science **309**, 1048 (2005).

[11] A. C. Fang, L. Capriotti, D. J. Scalapino, S. A. Kivelson, N. Kaneko, M. Greven, and A. Kapitulnik, Phys. Rev. Lett. **96**, 017007 (2006).

[12] Kenjiro K. Gomes, Abhay N. Pasupathy, Aakash Pushp, Shimpei Ono, Yoichi Ando and Ali Yazdani, Nature **447**, 569 (2007).

[13] Y. Kohsaka, K. Iwaya, S. Satow, T. Hanaguri, M. Azuma, M. Takano and H. Takagi, Phys. Rev. Lett. **93**, 097004 (2004).

[14] T. Kato, S. Okitsu and H. Sakata, Phys. Rev. B **72**, 144518 (2005).

[15] P. M. Singer, A. W. Hunt, and T. Imai, Phys. Rev. Lett. **88**, 047602 (2002).

[16] P. M. Singer, T. Imai, F. C. Chou, K. Hirota, M. Takaba, T. Kakeshita, H. Eisaki and S. Uchida, Phys. Rev. B **72**, 014537 (2005).

[17] Wei Chen, Giniyat Khaliullin and Oleg P. Sushkov, Phys. Rev. B **80**, 094519 (2009).

[18] For a review of early results see L. Pintschovius, Phys. Stat. Solids (b) **242**, No. 1, 30 50 (2005).

[19] L. Pintschovius, D. Reznik and K. Yamada, Phys. Rev. B **74**, 174514 (2006).

[20] D. Reznik, Advances in Condensed Matter Physics **2010**, Article ID 523549 (2010).

[21] S. L. Chaplot, W. Reichardt, L. Pintschovius and N. Pyka, Phys. Rev. B **52**, 7230 (1995).

[22] D. Reznik, L. Pintschovius, M. Fujita, K. Yamada, G. D. Gu and J. M. Tranquada, Journal of Low Temperature Physics **147**, 353364 (2007)

[23] We note that the total phonon density of states[18,24] has a peak at 87 meV that is relatively insensitive to doping; however, it would require an unreasonable amount of polycrystalline material in our samples for that to provide an explanation. We cannot rule out a multi-phonon effect.

[24] R. J. McQueeney, J. L. Sarrao, P. G. Pagliuso, P. W. Stephens and R. Osborn, Phys. Rev. Lett. **87**, 077001 (2001).

[25] P.B. Allen, Solid State Commun. **14**, 937 (1974)

[26] G. Grimvall, The Electron-Phonon Interaction in Metals, Selected Topics in Solid State Physics, edited by E. Wohlfarth (North-Holland, New York, 1981).

[27] S. Ono, Seiki Komiya, and Yoichi Ando, Phys. Rev. B **75**, 024515 (2007).

[28] S. Uchida, T. Ido, H. Takagi, T. Arima, Y. Tokura and S. Tajima, Phys. Rev. B **43**, 7942 (1991).

[29] T. Yoshida, X. J. Zhou, K. Tanaka, W. L. Yang, Z. Hussain, Z.-X. Shen, A. Fujimori, S. Sahrakorpi, M. Lindroos, R. S. Markiewicz, A. Bansil, Seiki Komiya, Yoichi Ando, H. Eisaki, T. Kakeshita and S. Uchida, Phys. Rev. B **74**, 224510 (2006).

[30] Yoichi Ando, A. N. Lavrov, Seiki Komiya, Kouji Segawa and X. F. Sun, Phys. Rev. Lett. **87**, 017001 (2001).

[31] K. Yamada, C. H. Lee, K. Kurahashi, J. Wada, S. Wakimoto, S. Ueki, H. Kimura, Y. Endoh, S. Hosoya, G. Shirane, R. J. Birgeneau, M. Greven, M. A. Kastner, and Y. J. Kim, Phys. Rev. B **57**, 6165 (1998).

[32] J. R. Gregg and C. W. Myles, J. Phys. Chem. Solids **46**, 1305 (1985).

[33] A. Gȯbel, D.T.Wang, M. Cardona, L. Pintschovius, W. Reichardt, J. Kulda, N.M.Pyka, K.Itoh and E.E. Haller, Phys. Rev. B **58**, 10510 (1998).

[34] O. Rošch and O. Gunnarsson, Phys. Rev. Lett. **92**, 146403 (2004).

[35] D. Reznik, L. Pintschovius, M. Ito, S. Iikubo, M. Sato, H. Goka, M. Fujita, K. Yamada, G. D. Gu and J. M. Tranquada, Nature **440**, 1170 (2006).

[36] T. Yoshida, X J Zhou, D H Lu, Seiki Komiya, Yoichi Ando, H Eisaki, T Kakeshita, S Uchida, Z Hussain, Z-X Shen and A Fujimori, J. Phys.: Condens. Matter **19**, 125209 (2007).

[37] A. Ino, C. Kim, M. Nakamura, T. Yoshida, T. Mizokawa, A. Fujimori, Z.-X. Shen, T. Kakeshita, H. Eisaki and S. Uchida, Phys. Rev. B **65**, 094504 (2002).

[38] T. Valla, A. V. Fedorov, P. D. Johnson, Q. Li, G. D. Gu, and N. Koshizuka, Phys. Rev. Lett. **85**, 828 (2000).

[39] T. Yoshida, M. Hashimoto, S. Ideta, A. Fujimori, K. Tanaka, N. Mannella, Z. Hussain, Z.-X. Shen, M. Kubota, K. Ono, Seiki Komiya, Yoichi Ando, H. Eisaki and S. Uchida. Phys. Rev. Lett. **103**, 037004 (2009).

[40] X. J. Zhou, T. Yoshida, D.-H. Lee, W. L. Yang, V. Brouet, F. Zhou, W. X. Ti, J. W. Xiong, Z. X. Zhao, T. Sasagawa, T. Kakeshita, H. Eisaki, S. Uchida, A. Fujimori, Z. Hussain and Z.-X. Shen, Phys. Rev. Lett. **92**, 187001 (2004).

[41] W. Meevasana, X. J. Zhou, S. Sahrakorpi, W. S. Lee, W. L. Yang, K. Tanaka, N. Mannella, T. Yoshida, D. H. Lu, Y. L. Chen, R. H. He, Hsin Lin, S. Komiya, Y. Ando, F. Zhou, W. X. Ti, J. W. Xiong, Z. X. Zhao, T. Sasagawa, T. Kakeshita, K. Fujita, S. Uchida, H. Eisaki, A. Fujimori, Z. Hussain, R. S. Markiewicz, A. Bansil, N. Nagaosa, J. Zaanen, T. P. Devereaux and Z.-X. Shen, Phys. Rev. B **75**, 174506 (2007).

[42] A. F. Bangura, P. M. C. Rourke, T. M. Benseman, M. Matusiak, J. R. Cooper, N. E. Hussey and A. Carrington, Phys. Rev. B **82**, 140501(R) (2010).

[43] M. Plate, J. D. F. Mottershead, I. S. Elfimov, D. C. Peets, Ruixing Liang, D. A. Bonn, W. N. Hardy, S. Chiuzbaian, M. Falub, M. Shi, L. Patthey and A. Damascelli, Phys.

Rev. Lett. **95**, 077001 (2005).
[44] Michael J. O'Hara, Charles W. Myles, John D. Dow and Ronald D. Painter, J. Phys. Chem. Solids **42**, 1043 (1981).
[45] Sidney R. Nagel, A. Rahman and Gary S. Grest, Phys. Rev. Lett. **47**, 1665 (1981).
[46] Sajeev John, H. Sompolinsky and Michael J. Stephen, Phys. Rev. B **27**, 5592 (1983).
[47] Tal Schwartz, Guy Bartal, Shmuel Fishman and Mordechai Segev, Nature **446**, 52 (2007).
[48] W. K. Yeoh, B. Gault, X. Y. Cui, C. Zhu, M. P. Moody, L. Li, R. K. Zheng, W. X Li, X. L. Wang, S. X. Dou, G. L. Sun, C. T. Lin and S. P. Ringer, Phys. Rev. Lett. **106**, 247002 (2011).
[49] Eiji Kaneshita, Masanori Ichioka and Kazushige Machida, Phys. Rev. Lett. **88**, 115501 (2002).